Cleaner Engineering and Technology 26 (2025) 100965

Contents lists available at ScienceDirect

Cleaner Engineering and Technology

journal homepage: www.sciencedirect.com/journal/cleaner-engineering-and-technology

Comparative analysis of water injection and EGR effects on combustion, performance, and emission characteristics of a diesel engine using diesel-biodiesel blends

Maziyar Moeini Manesh [a], Alireza Shirneshan [a,b,*], Sobhan Emami [a,b]

[a] Department of Mechanical Engineering, Najafabad Branch, Islamic Azad University, Najafabad, Iran
[b] Aerospace and Energy Conversion Research Center, Najafabad Branch, Islamic Azad University, Najafabad, Iran

ARTICLE INFO

Keywords:
Water injection
Exhaust gas recirculation
Biodiesel
NOx
Water droplet diameter

ABSTRACT

The pollutants emitted from diesel engines, especially nitrogen oxides (NOx), are one of the fundamental challenges for designers and manufacturers of internal combustion engines. Exhaust gas recirculation (EGR) and water injection are two essential methods for reducing NOx emitted from the engine. The comparison of these two methods when simultaneously utilizing biodiesel in the engine can be considered the most significant gap in previous research. This study investigates the effects of water injection and EGR, along with the application of various diesel-biodiesel blends, on the performance, combustion, and NOx emissions of a Caterpillar 3401 diesel engine. The AVL Fire CFD software package was utilized along with a three-zone extended coherent flame combustion model and k-ζ-f turbulence model for evaluating the impacts of water injection at percentages of 15 %, 30 %, 45 %, and 60 %, and EGR at rates of 0 %, 10 %, 15 %, 20 %, and 25 % for the B0, B10, B20, and B50 (50 % diesel-50 % biodiesel) blends. According to the results, increasing water injection by up to 45 % reduces the maximum in-cylinder pressure by 4.4 % and engine power by 3.2 %–4.4 % for different fuel mixtures. However, a slight increase in power is observed when the water injection percentage reaches 60 %. Additionally, the specific fuel consumption (SFC) rises by 6.4 % for these mixtures. Similarly, as the EGR rate increases, the maximum in-cylinder pressure decreases by up to 5.5 %, with power declining by 3.5 %–4.3 %, comparable to the water injection scenario. The SFC also increases by 3.7 %–4.6 % across different fuel blends, though slightly less than with water injection. The results also reveal that a water injection of 60 % reduces specific NOx by about 57 %; furthermore, increasing the EGR rate to 25 % reduces nitrogen oxides by approximately 78 %. It was found that a 0.18 mm diameter is the most suitable for water droplets to reduce NOx emissions during water injection. Based on the results, considering both engine performance and the reduction of nitrogen oxides, the EGR method is recommended over water injection.

Symbols and abbreviations

NOx	Nitrogen oxides	HRR	Heat release rate
EGR	Exhaust gas recirculation	DWI	Direct water injection
B	Biodiesel	PWI	Port water injection
D	Diesel	WDE	Water-diesel emulsion
CA	Crank angle	SMD	Sauter mean diameter
TDC	Top dead center	CFM	Coherent flame model
bTDC	Before top dead center	aTDC	After top dead center
CFD	Computational fluid dynamics	ECFM3Z	Three-zone extended coherent flame model
SFC	Specific fuel consumption	IVC	Intake valve closing
ANOVA	Analysis of variance	EVO	Exhaust valve opening
Adj SS	Adjusted sums of squares	Adj MS	Adjusted mean squares

1. Introduction

In recent years, governments have imposed specific restrictions on the emissions of diesel engines. These standards have directed the industry towards researching and improving pollution control methods. Since the emissions of unburned hydrocarbons and carbon monoxide

* Corresponding author. Department of Mechanical Engineering, Najafabad Branch, Islamic Azad University, Najafabad, Iran.
E-mail address: alireza.shirneshan@iau.ac.ir (A. Shirneshan).

https://doi.org/10.1016/j.clet.2025.100965
Received 24 October 2024; Received in revised form 13 March 2025; Accepted 2 April 2025
Available online 4 April 2025

from diesel engines are relatively small, these engines with high thermal efficiency offer the advantage of energy conservation but also have drawbacks concerning nitrogen oxides (NOx) and particulate matter emissions (Fayad et al., 2022, 2023). Specifically, diesel engines produce higher NOx emissions than SI gasoline engines (Park et al., 2011; Şahin et al., 2014). Several research has been conducted to find methods for controlling and mitigating NOx emissions, including water injection, exhaust gas recirculation (EGR), and modifications to engine parameters (Plee et al., 1981; Ghaffarpour et al., 1996; Dodge et al., 1996).

EGR, which recirculates a portion of the exhaust gases back into the engine intake, is employed to dilute the air and reduce oxygen, thereby decreasing the NOx emissions. In this mechanism, some exhaust gases are returned to the engine to dilute the air and lower the combustion temperature. EGR effectively reduces NOx levels since NOx is formed at high combustion temperatures and near stoichiometric combustion conditions (Yasin et al., 2015).

Introducing additives such as acetophenone, diethyl ether, dibutyl ether, ethyl hexanol, ethyl hexanoic acid, benzyl alcohol, ethanol, and water can also help reduce emissions. Another promising technique for NOx reduction is water injection, which cools the combustion process and dilutes the air-fuel mixture. One of the benefits of water injection is its ability to reduce NOx emissions across the entire engine load range without adversely impacting PM emissions. Although inert, water absorbs heat as it vaporizes within the combustion cylinder, effectively lowering the local adiabatic flame temperature. This reduction in peak flame temperature leads to a decrease in NOx emissions (Tesfa et al., 2012).

The first water-based injection system involves directly injecting water into the combustion cylinder. The second system, direct water injection (DWI), uses emulsification, where water and fuel are mixed with surfactants in a specialized mixer. The third method is intake manifold water injection, called port water injection (PWI). PWI has been extensively studied due to its lower cost, simplicity, and ease of implementation. Recent research indicates that DWI offers more significant potential for reducing emissions compared to PWI. The water-diesel emulsion (WDE) method also decreases harmful emissions and improves energy efficiency without modifying the diesel engine's internal structure (Zhang et al., 2019; Sun et al., 2022).

The practical application of water injection in diesel engines lies in its ability to enhance combustion efficiency, reduce nitrogen oxide (NOx) emissions, and suppress knocking tendencies. The precise water injection ratios significantly influence engine performance, demonstrating a notable reduction in combustion temperature and exhaust emissions. Furthermore, the findings provide insights into optimizing water injection systems, highlighting the potential for integrating this technology into modern diesel engines to comply with stringent emission regulations. These achievements validate the feasibility of water injection and open avenues for its adoption in sustainable automotive applications (Taghavifar et al., 2017).

Using biofuels like biodiesel has notably reduced carbon monoxide and unburned hydrocarbon emissions (Wei et al., 2022). However, one of the significant challenges associated with biodiesel usage in diesel engines is the increase in nitrogen oxides emissions (Hoekman et al., 2012). The elevated NOx emissions from biodiesel combustion are primarily attributed to the fuel's higher oxygen content, which leads to increased combustion temperatures (Giakoumis et al., 2012). Therefore, there is a severe concern regarding NOx emissions exceeding permissible limits when using biodiesel.

Various studies have explored strategies to mitigate NOx emissions while maintaining the environmental benefits of biodiesel.

In the field of exhaust gas recirculation, several studies have been made to investigate performance and NOx emissions from diesel engines. Yasin et al. (2015) investigated the effects of EGR combined with palm biodiesel on a Mitsubishi 4D68 engine and found that while NOx emissions decreased, engine power and torque were negatively affected. Zhou et al. (2015) conducted a numerical study on the impact of EGR on knocking phenomena in an RCCI engine using biodiesel-methanol blends, highlighting that proper control of EGR rates is crucial for optimizing performance and emissions. Similarly, Kumar et al. (2018) conducted a numerical study on varying EGR rates and their effect on NOx reduction, reporting up to 88 % reduction at a 25 % EGR rate. Combining biodiesel with other additives has also been explored as a potential solution for emission control. In another experimental study, Ergen (2024) investigated the use of diethyl ether with biodiesel in conjunction with EGR, achieving a significant reduction in NOx emissions by up to 70 % while improving engine performance compared to diesel fuel. Dubey et al. (2022) indicated that the blend containing 35 % biodiesel and 15 % EGR significantly reduced NOx emissions and smoke levels compared to pure diesel while maintaining acceptable thermal efficiency.

Regarding the simultaneous use of other biofuels and EGR, Rajesh Kumar et al. (Rajesh Kumar et al., 2016) examined the effects of EGR, fuel injection timing, and the use of normal pentanol, dimethyl carbonate, and isobutanol on fuel consumption, NOx emissions from the engine. Their findings indicated that the optimal conditions for reducing NOx emissions occur with a high EGR rate and the latest injection timing. They also revealed that NOx emissions are elevated in n-pentanol/diesel blends.

Several researchers have examined water injection's impact on diesel engines. Chintala and Subramanian (Chintala et al., 2016) demonstrated that water addition improved thermal efficiency while reducing NOx, HC, CO, and soot emissions. Moreover, Tsefa et al. (Tesfa et al., 2012) and Ayhan and Ece (Ayhan et al., 2020) explored direct water injection strategies, demonstrating that a 50–61 % reduction in NOx emissions could be achieved without severely compromising engine performance. In another study by Chen et al. (2022), the mass values of 10–35 % and 29–51 % of the fuel mass were investigated as the optimal water mass values for the two strategies. They revealed that NOx emissions were reduced by up to 30 % in the single water injection strategy, while in the dual water injection strategy, NOx emissions decreased by up to 90 %.

In several studies, the effect of water injection on NOx emissions has been investigated numerically; for example, Taghavifar et al. (2017) numerically analyzed different water injection strategies and identified an optimal 15 % water injection rate for maximizing power and efficiency while minimizing NOx. In another study, Sandeep et al. (2019) investigated the impact of water injection in the manifold on reducing NOx emissions in a heavy-duty cylinder diesel engine using 1-D thermodynamic simulation and AVL BOOST. The results indicated that a 16 % water injection led to a 13 % reduction in NOx emissions. Moreover, Soni and Gupta (Soni et al., 2016) studied the impact of using a diesel-methanol fuel blend and water injection using AVL Fire software on NOx emissions in a diesel engine. Their research indicated that water injection could reduce nitrogen oxides by up to 95 %.

Additionally, concerns related to engine reliability of using a water-emulsified biodiesel-diesel blend in a diesel engine have been addressed by Patidar and Raheman (Kumar Patidar et al., 2020). They reported using the specified blend resulted in reductions of 17, 25, and 14 % for CO, HC, and NOx emissions, respectively, along with a slight increase in CO_2. Reversely, another study (Ayhan, 2020) has reported an increase in HC, CO, and smoke emissions with a distinctive reduction (56 %) in NOx emissions when applying biodiesel and water injection simultaneously.

The literature indicates that using water injection and EGR are effective strategies for reducing NOx emissions in diesel engines while maintaining acceptable performance metrics. Water injection, whether direct or intake manifold injection, significantly lowers combustion temperatures, leading to substantial reductions in NOx emissions, as demonstrated by studies showing up to 90 % reductions. At the same time, water injection can influence engine parameters such as brake power and specific fuel consumption. Similarly, EGR has been shown to achieve notable NOx reductions, with rates as high as 88 % depending on the EGR percentage, while also decreasing soot production.

Prolonged exposure to diesel engine NOx emissions above a certain

level harms human health, prompting stringent emission regulations to reduce these pollutants (Alahmer et al., 2010). In addition, the transportation sector is shifting toward increasing the share of biodiesel to meet stricter emissions regulations, as it has long been regarded as a promising alternative to fossil diesel, offering significant reductions in pollutant emissions while contributing to energy security and environmental sustainability (Zhang et al., 2021). For example, the European Fuel Quality Directive (2009/30/EC) allows using biodiesel in standard diesel blends. Euro 6.2 introduced more stringent emission testing, and the upcoming Euro 7 regulation will also further tighten pollutant limits, reinforcing the need for a higher share of biodiesel alternative fuels. However, the combustion characteristics of biodiesel further increase nitrogen oxide emissions, exacerbating environmental pollution problems. Therefore, studying and comparing a wide range of EGR and injection ratios of water into the engine cylinder as the famous methods for addressing the NOx emission issues with the application of biodiesel further enhances emissions control and performance optimization, highlighting their potential for meeting stringent environmental standards in diesel engines and can be considered as a major research gap. This research aims to investigate and compare the effects of EGR rate (0, 10, 15, 20, and 25 %) and water injection ratio (0, 15, 30, 45, and 60 %) on engine combustion, performance characteristics, and NOx emissions, with the simultaneous application of different diesel-biodiesel blends (B0, B10, B20, and B50) using AVL Fire software to simulate the combustion process.

2. Numerical modeling

In this study, considering the geometry of the piston head of a CAT3401 Caterpillar diesel engine and following the engine specifications provided in Table 1, the desired geometry was modeled in the ESE Diesel module using AVL Fire software.

Although in the present study, the combustion chamber geometry was considered in three dimensions, due to the symmetry of the geometry and the fact that the injector nozzle has six holes, only a 60° sector of the geometry was considered to reduce computational time. As shown in Fig. 1, the computational domain was covered with dynamic structured grids that adapt well to traveling pistons.

2.1. Governing equations

The conservation equations of mass, momentum, energy, and species describe the turbulent combustion flow in a diesel engine. Although the density is a function of temperature, given that the Mach number of the flow is less than 0.3, the flow can be approximated as incompressible with reasonable accuracy.

2.1.1. Turbulence model

In this study, the k-ζ-f model, used for predicting the effects of near-wall fluid flow in turbulent flows, has been employed for turbulence modeling (Co., 2014).

In this model, the balance equations for turbulent kinetic energy, k, and the dissipation rate of turbulent kinetic energy,ε, are expressed by the following relations:

Table 1
The engine specifications.

Engine model	Caterpillar 3401
Engine type	Direct injection four-stroke cycle diesel engine
Displacement	2.44 lit
Compression ratio	15:1
Connecting rod length	26.162 cm
Engine speed	1600 rpm
Start timing of fuel injection	9° bTDC
Start timing of water injection	70° bTDC
Mass of fuel injected per cycle	0.1622 g

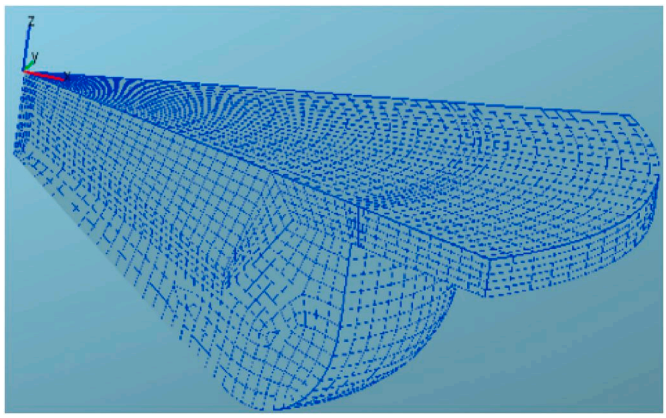

Fig. 1. 3D computational grid.

$$\frac{\partial k}{\partial t}+U_j\frac{\partial k}{\partial x_j}=P_k-\varepsilon+\frac{\partial}{\partial x_j}\left[\left(\nu+\frac{\nu_t}{\sigma_k}\right)\frac{\partial k}{\partial x_j}\right], \tag{1}$$

$$\frac{\partial \varepsilon}{\partial t}+U_j\frac{\partial \varepsilon}{\partial x_j}=\rho\left(\frac{C_{\varepsilon 1}P_k-C_{\varepsilon 2}\varepsilon}{\tau}\right)+\frac{\partial}{\partial x_j}\left[\left(\nu+\frac{\nu_t}{\sigma_\varepsilon}\right)\frac{\partial \varepsilon}{\partial x_j}\right]. \tag{2}$$

Additionally, the normalized velocity scale, ζ, is obtained from the following balance equation (Hanjalić et al., 2004):

$$\frac{\partial \zeta}{\partial t}+U_j\frac{\partial \zeta}{\partial x_j}=f-\frac{\varepsilon}{k}P_k+\frac{\partial}{\partial x_j}\left[\left(\nu+\frac{\nu_t}{\sigma_\zeta}\right)\frac{\partial \zeta}{\partial x_j}\right], \tag{3}$$

In the above equations, ν_t , U, ρ are molecular viscosity, turbulent viscosity, flow velocity, and density, respectively. Moreover, σ_k, σ_ε, σ_ζ, $C_{\varepsilon 1}$, and $C_{\varepsilon 2}$ represent the model constants.

The production term for turbulent kinetic energy, P_k, is expressed as follows:

$$P_k=\frac{\partial U_j}{\partial x_j}. \tag{4}$$

Equations (1)–(3) and an equation for the elliptic relaxation function f are solved. This equation is formulated using the Speziale-Sarkar-Gatski (SSG) pressure-strain correlation (Popovac et al., 2007):

$$L^2\nabla^2 f-f=\frac{1}{\tau}\left(C_1+C_2'\frac{P_k}{\varepsilon}\right)\left(\zeta-\frac{2}{3}\right)-\left(\frac{C_4}{3}-C_3\right)\frac{P_k}{k}, \tag{5}$$

In this relation, the time scale τ and the length scale L are obtained from the following equations:

$$\tau=max\left[min\left(\frac{k}{\varepsilon},\frac{0.6}{\sqrt{6}C_\mu|S|\zeta}\right),C_\tau\left(\frac{\nu}{\varepsilon}\right)^{1/2}\right], \tag{6}$$

$$L=C_L\,max\left[min\left(\frac{k^{3/2}}{\varepsilon},\frac{k^{1/2}}{\sqrt{6}C_\mu|S|\zeta}\right),C_\eta\left(\frac{\nu^3}{\varepsilon}\right)^{1/4}\right], \tag{7}$$

These time and length scales range from the Kolmogorov scales as the lower limit to Durbin's realisability constraints as the upper limit. The values of all model constants are reported in Table 2.

The mean strain rate, $|S|$, is obtained from the following equation:

$$|S|=\sqrt{S_{ij}S_{ij}}, \tag{8}$$

$$S_{ij}=\frac{1}{2}\left(\frac{\partial U_i}{\partial x_j}+\frac{\partial U_j}{\partial x_i}\right). \tag{9}$$

Finally, the turbulent viscosity is obtained from the following equation:

$$\nu_t=C_\mu\zeta k\tau. \tag{10}$$

Table 2
The k-ζ-f model coefficients (Popovac et al., 2007).

C_μ	$C_{\varepsilon 1}$	$C_{\varepsilon 2}$	C_1	C_2'	σ_k	σ_ε	σ_ζ	C_τ	C_L	C_η
0.22	$1.4(1 + 0.012/\zeta)$	1.9	0.4	0.65	1	1.3	1.2	6.0	0.36	85

2.1.2. Combustion model

Combustion modeling presents a fundamental challenge in the numerical simulation of turbulent reacting flows. Using a combustion model consistent with the considered problem's physics is essential. The most commonly used turbulent combustion model in numerical simulation of internal combustion engines is the Coherent Flame Model (CFM). This model assumes that the chemical time scale is much smaller than the turbulence time scale and can be neglected. In this model, the average flame speed and thickness, considered uniform along the flame front, depend solely on temperature, pressure, and the richness of unburned gases. Additionally, similar to all flamelet models, reactions are assumed to occur only in relatively thin layers that separate unburned from completely burned gases. Therefore, the average turbulent reaction rate is obtained from the product of the laminar burning velocity and the flame surface density (which indicates the degree of flame wrinkling) (Co., 2014).

The Coherent Flame Model itself consists of several sub-models; however, to model a diesel engine and the turbulent non-premixed combustion, as well as to implement the exhaust gas recirculation and to model pollutants (such as NOx), the three-zone Extended Coherent Flame Model (ECFM3Z) must be utilized. This model divides the combustion region into three zones: air, fuel, and fuel-air mixture (Co., 2014).

This combustion model is based on the flame surface density transport equation and a hybrid model capable of describing turbulent non-premixed and pre-mixed combustion. A wave model is used to model droplet breakup (Gao et al., 2016). This standard model can accurately predict droplet breakup time, liquid length, and spray penetration, making it widely applicable in diesel engine simulations. The extended Zeldovich mechanism for modeling NOx formation was also employed (Zeldovich et al., 1947). The biodiesel fuel considered in this study is FAME-R biodiesel, and the fuel blends are selected as percentages. The biodiesel properties according to ASTM D6751 standard are presented in Table 3.

2.2. Grid study

Four different meshes, consisting of 7,440, 14,288, 20,724, and 32,193 cells, were selected and compared for the in-cylinder pressure parameter to conduct the grid convergence study, as shown in Fig. 2. According to the figure, the pressure variations for the grids with 14,288, 20,824, and 32,193 cell numbers showed nearly similar results and gave adequately grid-independent results. Therefore, the grid with 14,288 cells was selected as the mesh configuration for this study.

2.3. Model validation

The simulation results for the in-cylinder pressure were compared with experimental results from the research by Nehmer and Reitz (Nehmer et al., 1994) on neat diesel fuel to validate the proposed model (Fig. 3). Additionally, the model predicted NOx values expressed as NOx produced per unit of fuel consumed were compared with the results reported by Mobasheri et al. (2012) (Fig. 4). The figures demonstrate that the current numerical results are in good agreement with the results of the previous works, confirming the validity of the proposed model. The calculations were performed over a closed cycle to reduce simulation time, from the intake valve closing (IVC) at 190° CA to the exhaust valve opening (EVO) at 521° CA.

Table 3
Thermo-physical characteristics of the biodiesel.

Property	Units	Biodiesel
Lower heating value	MJ/kg	38.3
Cetane number	–	57
Density	g/cm^3	0.88
Kinematic viscosity	mm^2/s at 40 °C	4.43

3. Results and discussion

3.1. Effect of water injection on the temperature distribution inside the combustion chamber

Fig. 5 shows the temperature distribution inside the combustion chamber for cases without water injection and 60 % water injection using neat diesel fuel at various crankshaft angles. The water spray begins at 70° before the TDC, or in other words, at 290° CA, and ends at 310° CA.

As shown in the figure, the temperature in the combustion chamber decreases when water injection starts, with this cooling effect being most noticeable around the water nozzle. As water injection continues (at 310° CA), a larger combustion chamber area experiences a temperature drop. At 315° CA (i.e., 5° after the end of water injection), there is less water mass near the spray nozzle; however, water accumulation can be observed near the bottom of the piston bowl.

According to the figure, at 350° CA (5° after the start of fuel injection and 40° after the end of water injection), the results indicate that in the water spray case, many areas of the combustion chamber have experienced a decrease in temperature due to heat absorption by the water. At 360° CA, where fuel injection continues and the piston is at TDC, the temperature difference between the cases with and without water injection is visible. Since fuel injection ends at 366.5° CA, the temperature difference in various combustion chamber areas remains significant in the water spray case at 370° CA. The zone near the bottom of the piston bowl and close to the walls of the combustion chamber exhibits the most remarkable temperature differences. At 377° CA, it is observed that for the two spray conditions-water spray and no water spray-the temperature difference has minimized, and the corresponding areas of the chamber have almost the same temperature. This behavior occurs because the effect of water spraying at this stage of the cycle is less than in the previous stage due to the dominance of very high temperatures resulting from the combustion process, which diminishes the cooling effect of the water spray.

3.2. Effect of water droplet diameter on water distribution and NOx emission

As observed in the previous section, water injection significantly affects temperature distribution within the cylinder. The penetration depth of water droplets and their distribution inside the cylinder can be influenced by droplet diameter and the spray cone angle. To examine the effect of droplet diameter on the water distribution, the contour of the water mass fraction inside the cylinder for three droplet diameters-0.14 mm, 0.18 mm, and 0.259 mm-has been presented at various crankshaft angles in Fig. 6. The water mass fraction in these figures is 60 %, and the spray cone angle is 8°. An equal water mass of 97.32 mg per cycle is injected in all three cases.

According to the results, at 295° CA, which is 5° after water injection

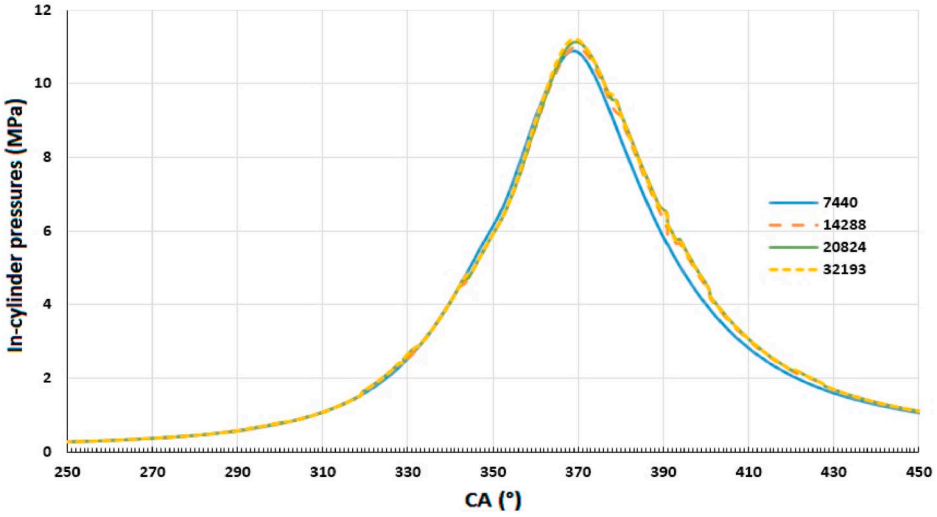

Fig. 2. Grid independent results.

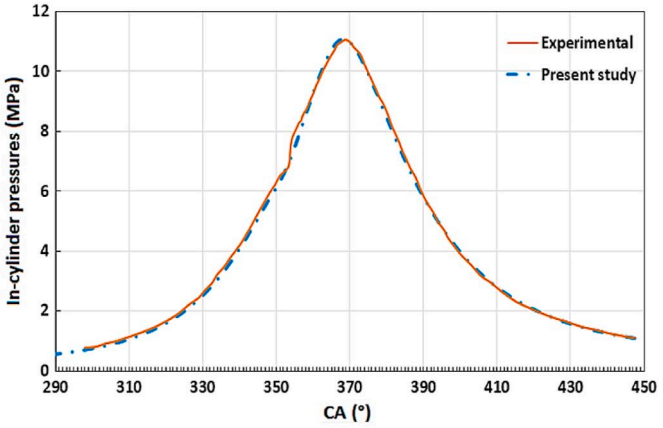

Fig. 3. The numerical and experimental (Nehmer et al., 1994) results of In-cylinder pressure.

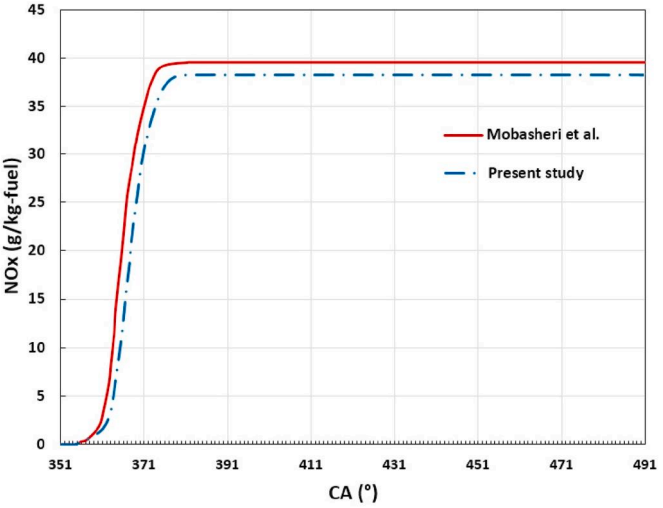

Fig. 4. The Predicated NOx in comparison with the previous research (Mobasheri et al., 2012).

starts this crankshaft angle, the water mass fraction for a droplet diameter of 0.14 mm is higher than droplet diameters of 0.18 mm and 0.259 mm. Moreover, smaller droplets cover a wider area with greater penetration depth. This observation also holds for 300° and 310° CA. It appears that with an increase in droplet diameter and consequently an increase in the drag force acting on the droplets, the spray penetration length and the depth of the droplet throw toward the piston bowl decrease.

Fig. 7 shows the effect of droplet diameter on specific NOx emissions. This parameter essentially measures the amount of nitrogen oxides emitted per unit of engine power output. Since the droplet diameter affects the distribution of the water mass fraction in the chamber, it can be concluded that this variable also influences the temperature distribution in the chamber and NOx emissions.

The Figure illustrates that as the droplet diameter of the sprayed water changes, the amount of nitrogen oxides emitted per unit of engine power also varies. According to the figure, the specific NOx emission decreases as the spray nozzle diameter increases from 0.14 mm to 0.18 mm but then increases from 0.18 mm to 0.26 mm. This behavior could be attributed to the fact that the initial effect of water spray is highest for the nozzle hole diameter of 0.18 mm compared to 0.14 mm, resulting from the increased spray penetration length with the higher diameter (Moon et al., 2010). Subsequently, the water evaporation characteristics are primarily influenced by the Sauter mean diameter (SMD) of the water droplets; a higher SMD of droplets leads to lower water evaporation (Farnham et al., 2015; Raut et al., 2019), resulting in higher specific NOx emissions. Therefore, the optimal nozzle diameter among the examined options is 0.18 mm, at which the specific NOx emission reaches its minimum value of 0.24 gr/kW·hr.

3.3. *Effect of spray cone angle on water distribution and NOx emission*

The water distribution inside the cylinder for spray angles of 8, 12, and 16° is illustrated in Fig. 8 to show the effect of the spray cone angle on water distribution. In these images, the water mass fraction and the droplet diameter are set at 60 % and 0.26 mm, respectively. An equal water mass of 97.32 mg per cycle is injected in all three cases.

According to Fig. 8, at 300° CA, the penetration length of the water spray at an angle of 8° is higher than in the cases of 12 and 16°. Additionally, the water concentration at the 8-degree angle extends over a longer distance compared to the other two cases.

Fig. 8 also shows the water mass fraction distribution at 310° CA, the end angle of water injection. In this case, the penetration length at 8° is higher than at the other angles, with more water observed on the piston

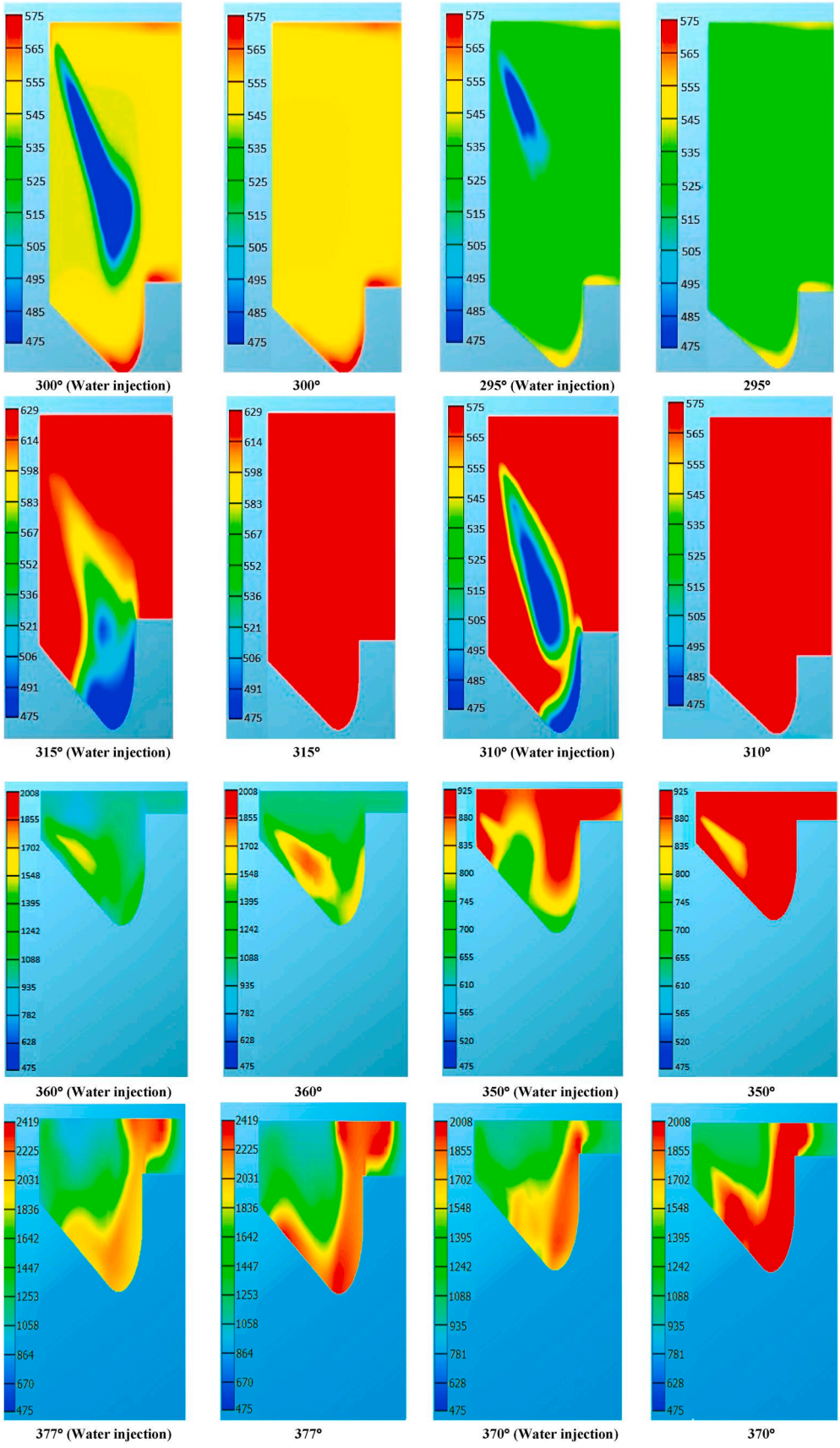

Fig. 5. Temperature contour inside the cylinder at different CAs in the state without injection and with water injection.

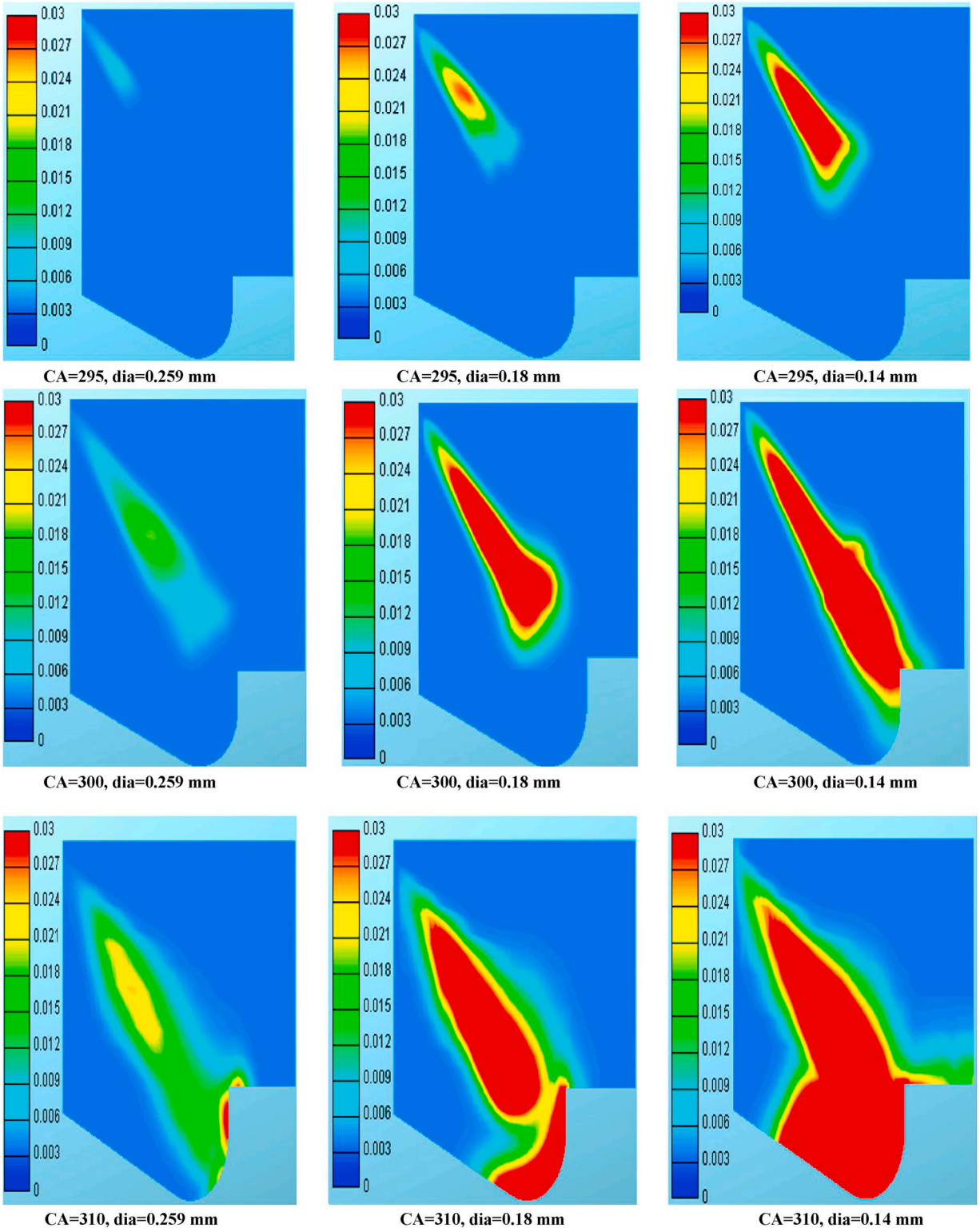

Fig. 6. H_2O mass fraction contour inside the cylinder with a droplet diameter of 0.14, 0.18, and 0.26 mm.

bowl and some on the piston crown. It can be asserted that the spray cone angle significantly influences the distribution of the water mass fraction within the combustion chamber and the extent, width, and penetration depth of the sprayed water.

Fig. 9 shows the effect of the spray angle on specific NOx emissions. Since the spray angle affects the distribution of the water mass fraction in the chamber, it can be concluded that this variable also impacts the temperature distribution in the chamber and the emission of nitrogen oxides.

The figure shows that as the spray angle of the injected water changes, the amount of nitrogen oxides emitted per unit of engine power also varies. According to the figure, the specific NOx emissions decrease nearly linearly as the spray angle increases from 8 to 16°. With an increase in the spray cone angle, despite a shorter penetration length, a

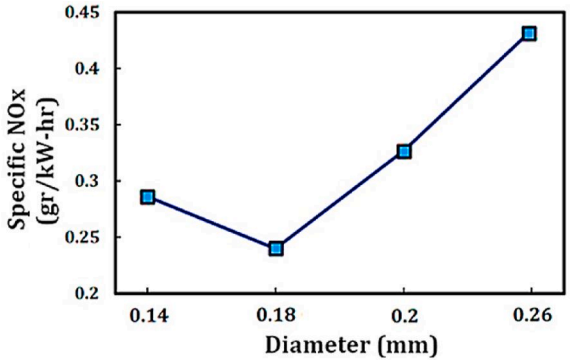

Fig. 7. Variation of specific NOx with droplets diameter of injected water.

larger volume and area of the field are affected by the water droplets, resulting in lower NOx emissions; at a spray angle of 16°, the specific NOx emission reaches 0.364 gr/kW·hr.

3.4. *Effect of water injection and biodiesel percentage in the fuel mixture on engine combustion and performance characteristics*

3.4.1. *In-cylinder pressure*

Figs. 10–12 show the in-cylinder pressure diagrams for different water injection percentages and diesel-biodiesel mixtures.

Based on the results, increasing the water injection percentage reduces in-cylinder pressure at various crankshaft angles for all fuel mixtures. The highest pressure is observed without water injection, while the lowest pressure occurs with 45 %. This trend is due to the decrease in combustion temperature caused by water injection during the compression phase, which reduces the pressure inside the engine's combustion chamber. The figures show that in all water injection cases, the peak in-cylinder pressure shifts to later due to the increased ignition delay caused by water injection. In the case of 60 % water injection, the higher amount of water vapor leads to higher pressure, with the rate of this increase becoming more pronounced as water injection and evaporation intensify. Conversely, in low water injection cases, the primary effect is cooling, which disrupts effective ignition and complete combustion. As a result, the peak in-cylinder pressure for low water injection cases is lower than the baseline diesel operation (Taghavifar et al., 2019). According to the results, the maximum in-cylinder pressure decreases by up to 4.4 % compared to the case without water injection. Additionally, the results show that as the biodiesel percentage in the fuel mixture increases, the combustion pressure slightly rises. This behavior can be attributed to the higher complete combustion of biodiesel due to a shorter ignition delay and the presence of oxygen molecules in its structure (Shirneshan et al., 2014).

3.4.2. *Heat release rate (HRR)*

Figs. 13–15 show the heat release rate diagrams for different water injection percentages and diesel-biodiesel mixtures.

Based on the results, the heat release rate generally decreases after water injection, although the peak heat release rate increases for a water injection ratio of 60 %. Additionally, combustion starts later in cases with water injection, with this delay being more pronounced in the 45 % water injection case. It can be observed that the peak of the heat release rate occurs further from the TDC in the water injection cases, indicating a higher ignition delay in comparison to the case without water injection. The cooling effect of water on the inlet air temperature causes the

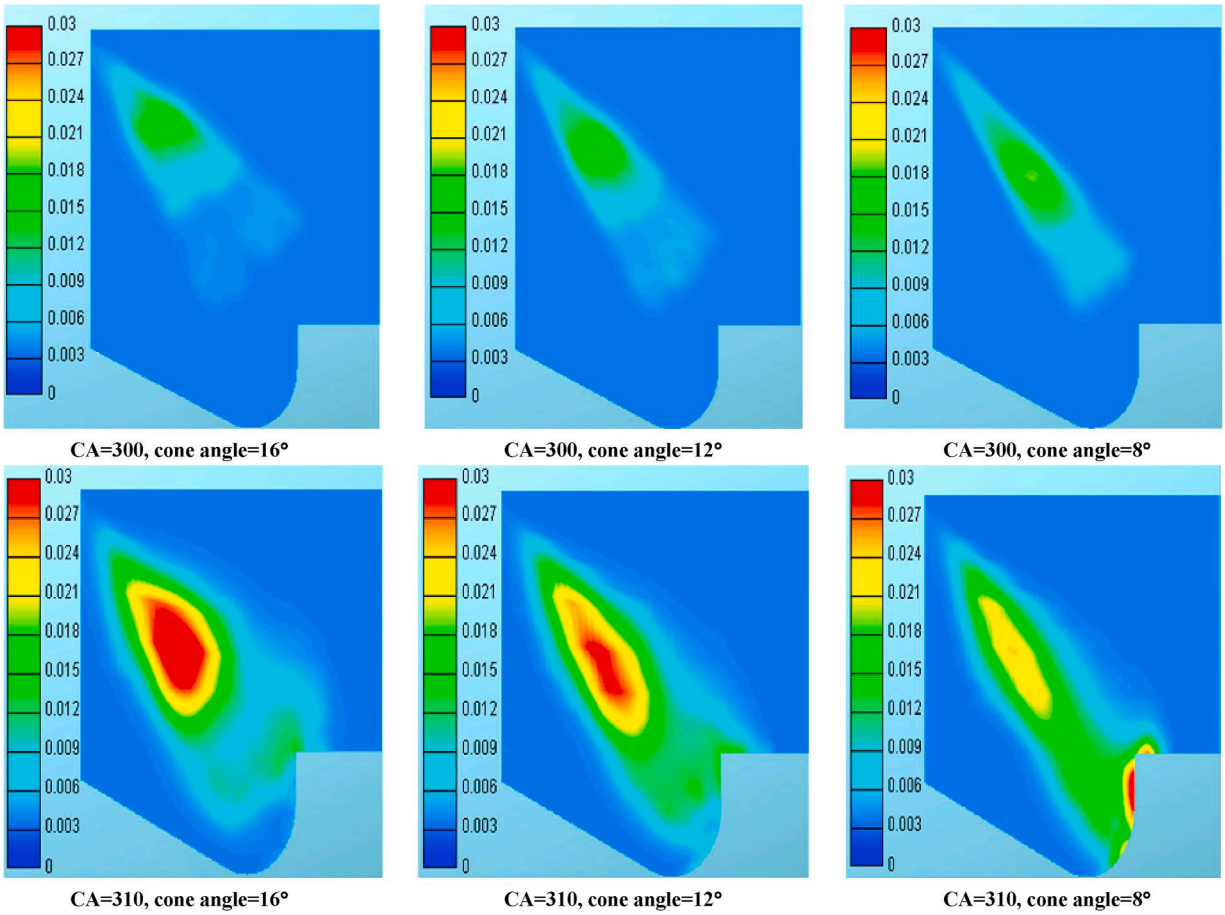

Fig. 8. H_2O mass fraction contour inside the cylinder for water spray with conical angles of 8, 12, and 16°.

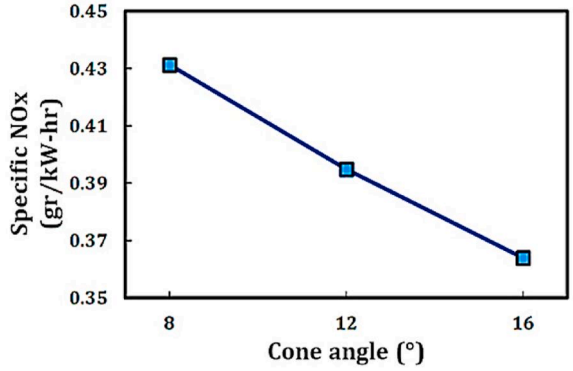

Fig. 9. Variation of specific NOx with a cone angle of injected water.

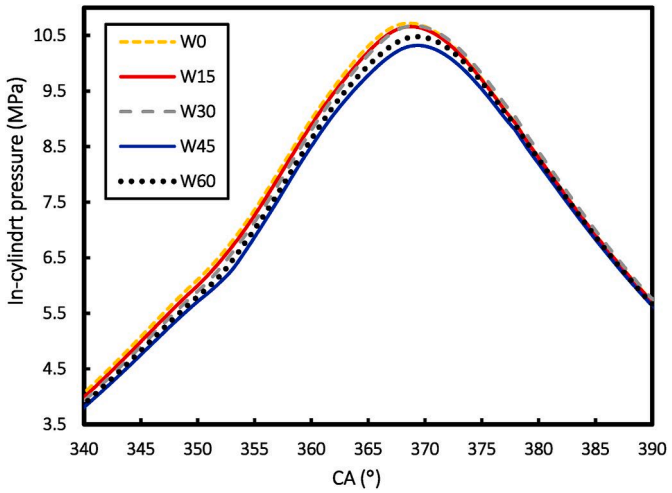

Fig. 10. In-cylinder pressure diagram for neat diesel and different water injection percentages.

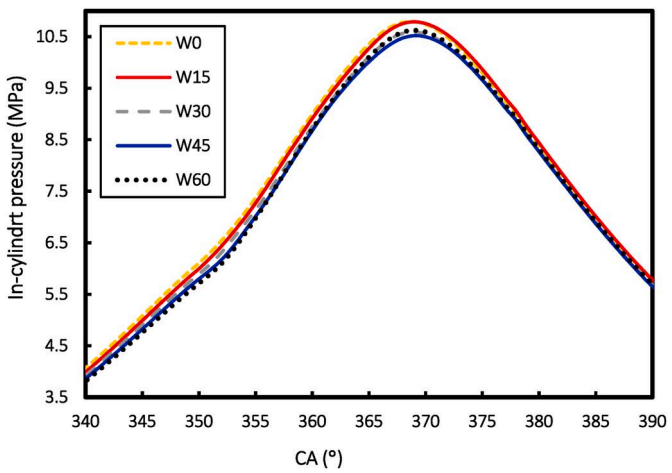

Fig. 11. In-cylinder pressure diagram for B20D80 and different water injection percentages.

ignition delay (Tesfa et al., 2012). A diesel engine's ignition delay generally includes physical and chemical ignition delays. The physical ignition delay significantly influences the overall ignition delay (Zhang et al., 2019). Although the ignition delay increased significantly, likely due to the latent heat of vaporization of water and its higher viscosity, the extended ignition delay can enhance the physical evaporation and

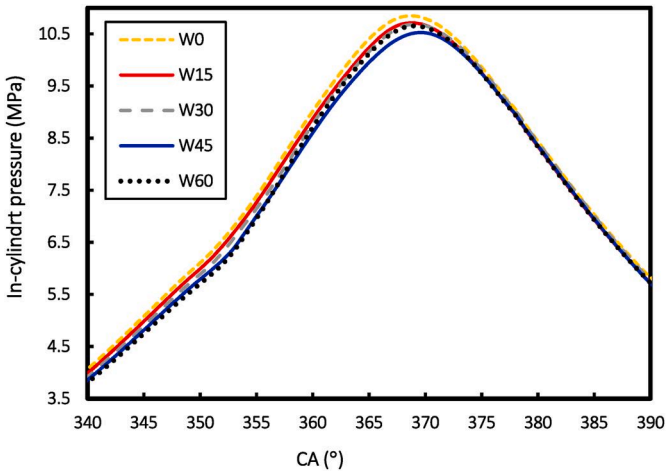

Fig. 12. In-cylinder pressure diagram for B50580 and different water injection percentages.

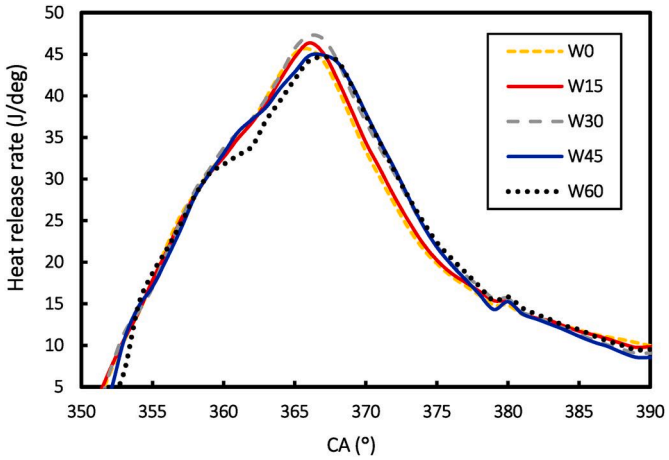

Fig. 13. Heat release rate diagram for neat diesel and different water injection percentages.

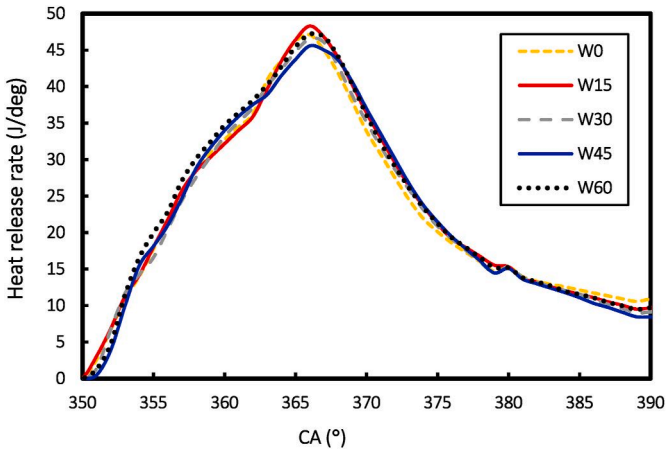

Fig. 14. Heat release rate diagram for B20D80 and different water injection percentages.

air-fuel mixing process within the cylinder, particularly in the case of 60 % water injection (Zhang et al., 2019).

Additionally, the addition of water to the fuel induces the micro-explosion phenomenon. This phenomenon enhances the exposure of

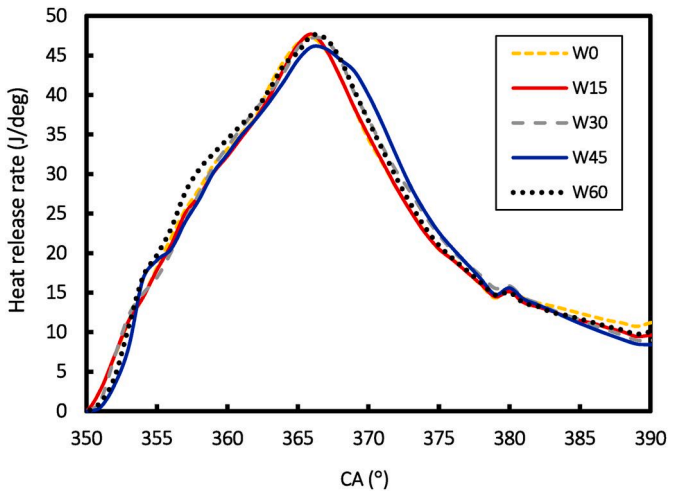

Fig. 15. Heat release rate diagram for B50D50 and different water injection percentages.

the injected fuel to oxygen, leading to improved combustion. The effect becomes more pronounced with higher water content, particularly in the case of 60 % water injection (Tesfa et al., 2012; Zhang et al., 2019). Micro-explosions of water vapor near diesel fuel significantly accelerate the mixing of diesel fuel and air, which is crucial for the combustion process in a diesel engine, as it relies on rapid and homogeneous air-fuel mixing (Şahin et al., 2014; Taghavifar et al., 2019). Thus, micro-explosions are considered secondary atomization, where droplet sizes are significantly reduced, leading to improved air-fuel mixing. In addition, adding water can also significantly impact the chemical kinetics within the combustion chamber (Tesfa et al., 2012). As a result, at crankshaft angles after 365°, the heat release rate slightly increases for water injection cases.

The results also show that the heat release rate slightly increases with increased biodiesel percentage in the fuel mixture. This increase can be attributed to the presence of oxygen in the molecular structure of biodiesel and a shorter ignition delay in biodiesel-containing fuels, leading to more complete and prolonged combustion, compensating for its lower calorific value compared to diesel (Zhang et al., 2021). Based on the results, it is observed that the heat release rate slightly increases near a crankshaft angle of 380°, which can be attributed to the ignition of unburned fuel remaining in the combustion chamber.

3.4.3. Engine power

Fig. 16 shows the engine power values for various water injection percentages and diesel-biodiesel mixtures.

According to the results, engine power decreases by 3.2 %–4.4 % on average for different fuel mixtures as the water injection percentage increases from 0 % to 45 %. Water injection in the combustion process of a diesel engine can lead to reduced engine power due to several factors. The vaporization of water absorbs heat, lowering peak combustion temperatures and reducing the efficiency of fuel burning. This cooling effect also dilutes the air-fuel mixture, decreases oxygen availability, and delays ignition, all weakening combustion. Moreover, some energy is diverted to vaporize the water rather than contribute to power generation (Sun et al., 2022; Raut et al., 2019). However, the power slightly increases when the water injection percentage reaches 60 %. This increase may be attributed to droplet micro-explosions and the vapor fraction in the mixture resulting from adding water, which can enhance atomization and mixing properties, significantly contributing to uniformity, improved combustion efficiency, and increased engine power (Zhang et al., 2019; Taghavifar et al., 2019).

Additionally, the results show that engine power slightly rises as the biodiesel percentage in the fuel mixture increases. This increase can be due to the more complete combustion of biodiesel, owing to the presence of oxygen molecules in its structure and its shorter ignition delay.

3.4.4. Specific fuel consumption

Fig. 17 shows the specific fuel consumption values of the engine for different water injection percentages and various diesel-biodiesel mixtures.

According to the results, as the water injection percentage increases from 0 % to 45 %, the specific fuel consumption increases by 6.8 % on average for different fuel mixtures. This result could be due to various factors. The cooling effect of water vaporization lowers combustion temperatures, reducing thermal efficiency and requiring more fuel to maintain the desired power output. Additionally, the dilution of the air-fuel mixture and reduced oxygen availability lead to incomplete combustion, necessitating increased fuel input to compensate for the loss of efficiency. Water injection also delays the ignition process, disrupting optimal combustion timing and reducing the overall energy release from the fuel.

Furthermore, the energy absorbed by water during vaporization does not contribute to useful work, resulting in higher fuel consumption to achieve the same power output. These combined effects increase the engine's SFC (Sandeep et al., 2019; Taghavifar et al., 2019). However, as the water injection percentage rises from 45 % to 60 %, the specific fuel consumption slightly decreases. This increase may be attributed to the higher power achieved with a 60 % water injection ratio.

The results indicate that increasing the biodiesel percentage in the fuel mixture does not lead to significant changes in specific fuel consumption. However, this parameter increases slightly for B50 due to the higher density of biodiesel than diesel (Shirneshan et al., 2014).

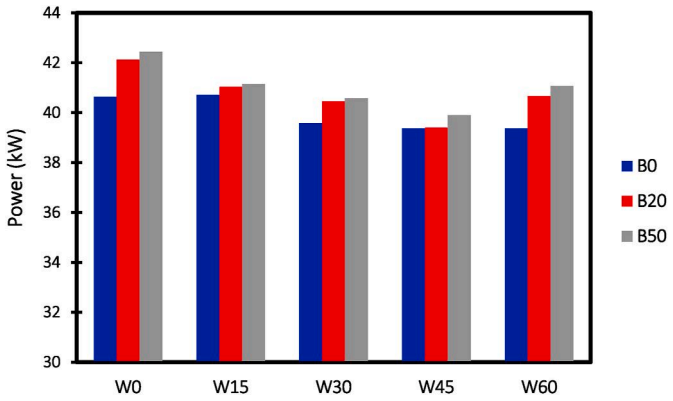

Fig. 16. Indicated power values for different water injection percentages and diesel-biodiesel blends.

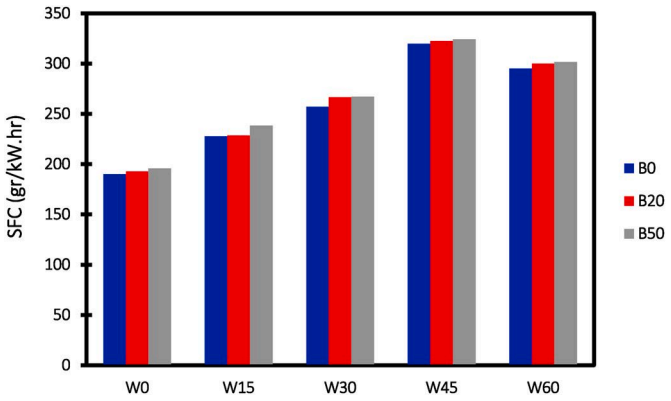

Fig. 17. Specific fuel consumption values for different water injection percentages and diesel-biodiesel blends.

3.5. Effect of EGR and biodiesel percentage in the fuel mixture on engine combustion and performance characteristics

3.5.1. In-cylinder pressure

Figs. 18–20 show the In-cylinder pressure diagrams for different EGR rates and diesel-biodiesel mixtures.

Based on the results, the pressure at various crankshaft angles decreases as the EGR rate increases for all fuel mixtures. The figures show that the peak combustion pressure decreased as the EGR ratio increased. This trend can be attributed to several factors. Firstly, a higher EGR ratio increases the volume fraction of CO_2 in the cylinder, which dilutes the mixture and reduces the chemical reaction rate. Additionally, the chemical effects of CO_2 can suppress or alter the chemical equilibrium, thereby limiting the heat released during the reaction process. Moreover, introducing EGR affects both the combustion rate and combustion efficiency. Consequently, the in-cylinder mean temperature decreases with a higher EGR ratio, reducing the peak combustion pressure (Duan et al., 2021). Moreover, applying EGR to the engine reduces cylinder pressure values due to decreased oxygen in the combustion chamber (Ergen, 2024). The results indicate that the maximum in-cylinder pressure decreases by 5.5 % compared to the case without EGR for different fuel mixtures. Additionally, the in-cylinder pressure values with EGR are higher than those with water injection. Similarly, the results show that as the biodiesel percentage in the fuel mixture increases, the maximum combustion pressure slightly increases.

3.5.2. Heat release rate (HRR)

Figs. 21–23 show the heat release rate diagrams for various EGR rates and diesel-biodiesel blends.

The results indicate that the heat release rate generally decreases with an increase in the EGR rate. This trend is particularly pronounced around 5° aTDC, primarily due to the temperature-lowering effect of EGR, the dilution of intake air, the reduced availability of oxygen for combustion, and the absorption of combustion heat during the initial stages. Introducing gases with high specific heat capacity through EGR reduces the heat release rate (Rajesh Kumar et al., 2016; Ramesh et al., 2017). However, at an EGR rate of 25 %, the heat release rate decreases significantly due to the thermal and dilution effects caused by the high volume of recirculated exhaust gases. Furthermore, the increased EGR rate reduces the oxygen concentration in the combustion chamber, leading to an extended ignition delay period. As a result, the peak HRR is significantly delayed, moving further away from the TDC (Ramesh et al., 2017).

The results show that the maximum heat release rate with EGR is reduced by 9.5 % compared to the case without EGR, which is a higher reduction than water injection. In this case, similar to the water injection scenario, the heat release rate rises slightly near 380° CA, which can be attributed to the ignition of unburned fuel remaining in the engine's combustion chamber. Furthermore, the results indicate that, similar to the water injection case, the heat release rate increases as the percentage of biodiesel in the fuel blend increases.

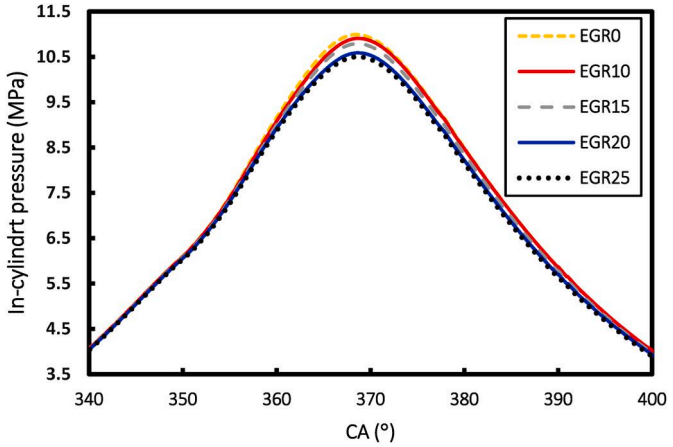

Fig. 18. In-cylinder pressure diagram for neat diesel and different EGR rates.

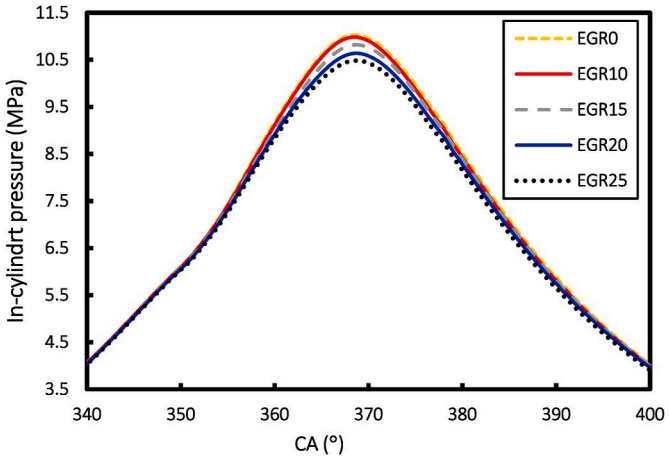

Fig. 19. In-cylinder pressure diagram for B20D80 and different EGR rates.

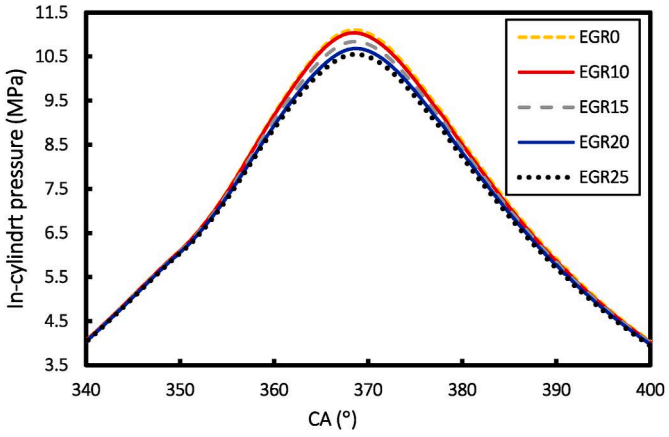

Fig. 20. In-cylinder pressure diagram for B5050 and different EGR rates.

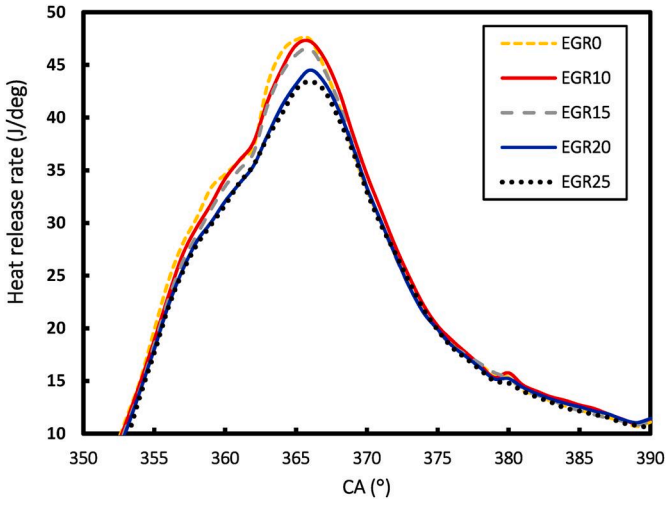

Fig. 21. The heat release rate for pure diesel and different EGR rates.

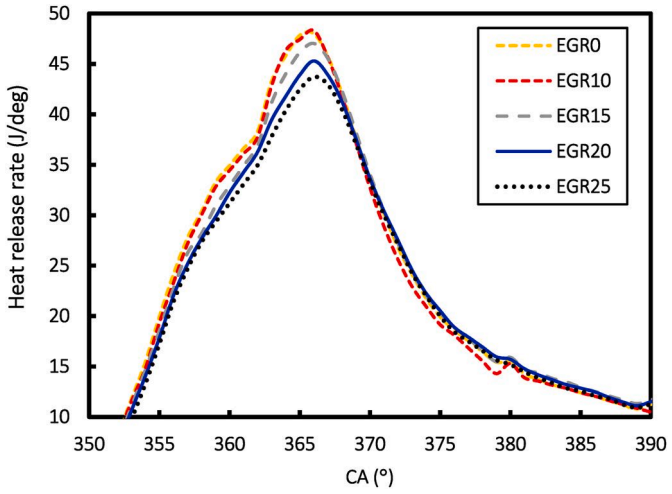

Fig. 22. The heat release rate for B20D80 and different EGR rates.

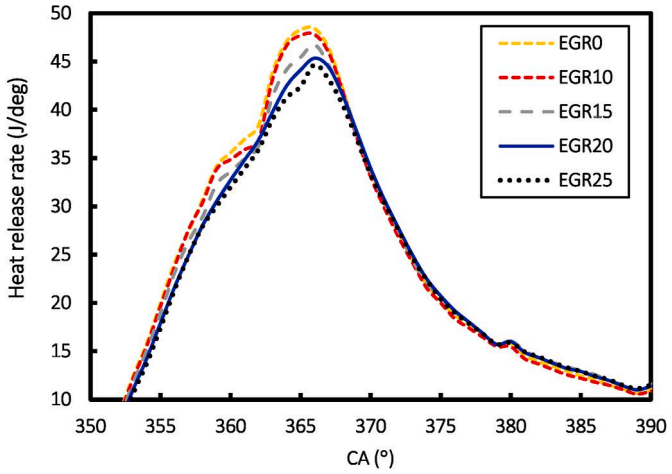

Fig. 23. The heat release rate for B50580 and different EGR rates.

3.5.3. Engine power

Fig. 24 shows the indicated power values of the engine for various EGR rates and different diesel-biodiesel blends. According to the results, the indicated power decreases as the EGR rate increases from 0 % to 25 %. This decrease is attributed to the reduced pressure generated during the power stroke and the lower oxygen content in the cylinder caused by the introduction of exhaust gases, which reduces the engine's power output (Rajesh Kumar et al., 2016). Similar to the case of water injection, the power output of the fuel blend increases with a higher proportion of biodiesel. The highest indicated power is observed with a fuel mixture containing 50 % biodiesel and no EGR, while the lowest value is associated with 25 % EGR for pure diesel fuel. The results also indicate that EGR's power values are higher than water injection's. However, as the EGR rate increases across different fuel blends, the power decreases by 3.5 %–4.3 %, roughly similar to the water injection scenario.

3.5.4. Specific fuel consumption

Fig. 25 shows the SFC values for various EGR rates and diesel-biodiesel blends.

According to the results, as the EGR rate increases, the specific fuel consumption rises by 3.7 %–4.6 % for different fuel blends. This behavior is due to the reduction in combustion quality caused by the chemical effects of the inert gases in the EGR and the decreased oxygen molecules inside the combustion chamber, which worsens oxidation reactions and engine performance (Radheshyam et al., 2020). Moreover, the introduction of EGR raises the specific heat capacity of the combustible content, which lowers the combustion temperature. These conditions, in turn, reduce the flame propagation speed and increase the likelihood of misfire. Consequently, more fuel is required to maintain and improve combustion quality (De Poures et al., 2017; Qi et al., 2021). According to the results, the specific fuel consumption with EGR is slightly lower than that of the water injection scenario. The results also show that as the biodiesel percentage increases, the specific fuel consumption increases due to biodiesel's higher density and lower heating value than pure diesel (Shirneshan et al., 2014; Hojati et al., 2019). The highest specific fuel consumption is observed with a 25 % EGR rate and the B50 blend, while the lowest consumption corresponds to pure diesel without EGR.

3.6. Specific NOx emissions

3.6.1. The effect of water injection ratio and the percentage of biodiesel in the fuel blend

Fig. 26 shows the specific NOx emission for various water injection percentages, ranging from 0 to 60 %, and different biodiesel-diesel blends from B0 to B50.

According to Fig. 26, as the water injection percentage increases from 0 % to 60 %, the NOx emissions decrease by an average of up to 57 %. The highest NOx level occurs for 0 % water injection and B50 blend with 0.5985 g/kWh. Conversely, 60 % water injection and pure diesel fuel with 0.24 g/kWh have the lowest NOx level. The reduction in NOx with increased water injection volume is attributed to decreased peak temperatures within the combustion chamber. The reduction of ignition delay minimizes the reaction time of the free nitrogen and oxygen gas in the combustion cylinder, which is the primary mechanism of NOx

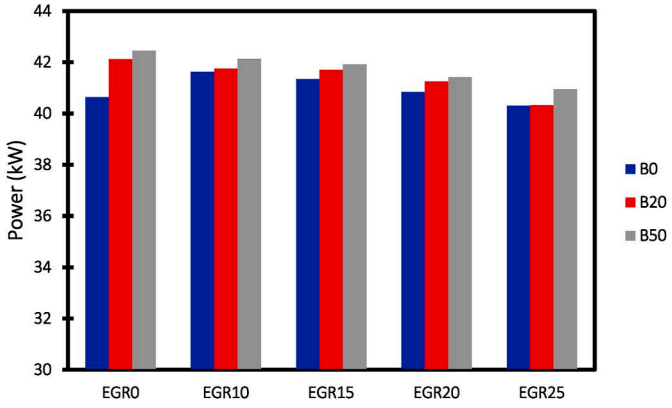

Fig. 24. Indicated power diagram for various EGR rates and diesel-biodiesel blends.

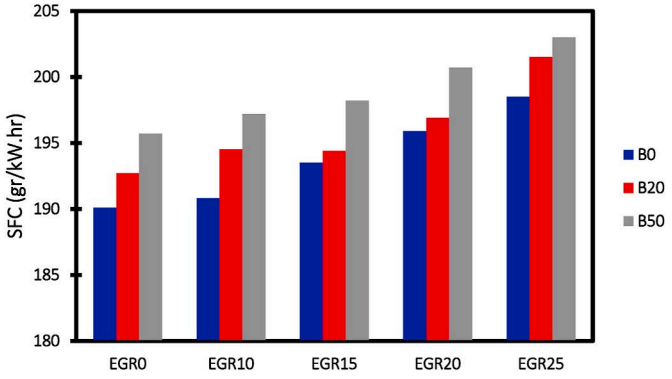

Fig. 25. Specific fuel consumption diagrams for various EGR rates and diesel-biodiesel blends.

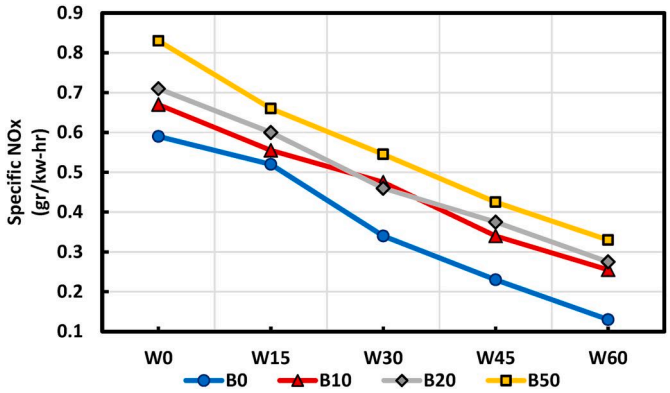

Fig. 26. Variation of specific NOx against the water percentage injection for different biodiesel-diesel blends.

formation. The results show that NOx emission decreases proportionally when the water ratio increases. The reason is that when water is injected into the cylinder, it absorbs some heat during the vaporization process. The process reduces the combustion chamber's peak flame temperature, which negatively impacts the formation of NOx emissions. Furthermore, water injection into the cylinder changes the thermo-physical properties of water, affecting the gas mixture's heat transfer coefficient and facilitating heat loss through the cylinder walls (Tesfa et al., 2012).

Additionally, the figure indicates that as the share of biodiesel in the fuel blend increases, NOx emissions rise for all water injection amounts. This increase is due to the presence of oxygen molecules in the structure of biodiesel, which contributes to higher nitrogen oxide production. Moreover, a higher percentage of biodiesel results in improved combustion, or in other words, a cleaner burn, leading to higher heat release. As biodiesel content increases from 0 % to 50 %, NOx emissions increase by approximately 17 %.

3.6.2. The effect of EGR rate and the percentage of biodiesel in the fuel blend on NOx emissions

The formation of nitrogen oxides depends on three key factors: high in-cylinder temperatures, a high concentration of oxygen, and extended reaction residence time (Kumar et al., 2018). Fig. 27 shows the specific NOx emission for various EGR rates, ranging from 0 % to 25 %, and different biodiesel-diesel blends from B0 to B50.

The results indicate that EGR significantly reduces NO emissions as the EGR rate increases from 0 % to 25 %, primarily due to a decrease in in-cylinder temperature. This reduction occurs because the use of EGR lowers the mean combustion temperature. As previously mentioned, the formation of NOx emissions within the cylinder is strongly influenced by combustion temperature. Lowering the temperature increases the activation energy needed for NOx formation reactions, effectively reducing NOx emissions in the combustion chamber (Duan et al., 2021). The highest NOx level occurs at 0 % EGR and B50 with 0.823 g/kWh. Conversely, the lowest NOx level (0.132 g/kWh) belongs to 25 % EGR and B0. However, as the EGR rate increases from 0 % to 25 %, NOx emissions, on average, decrease by approximately 78 %. Moreover, the NOx increases up to 19 % as the biodiesel percentage increases in the fuel mixture.

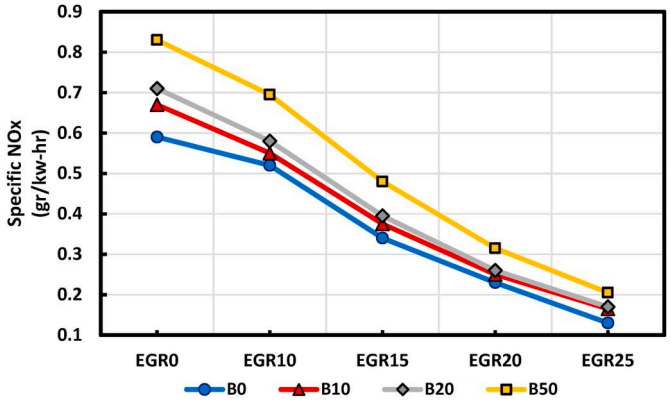

Fig. 27. Variation of specific NOx against the EGR ratio for different biodiesel-diesel blends.

3.7. Statistical analysis

A two-way ANOVA has been performed to evaluate the effectiveness of the independent variables (water injection ratios, EGR rates, and biodiesel proportion in the fuel mixture) on the dependent variables (output power, SFC, and NOx emissions), as presented in Tables 4 and 5.

According to Table 4, the results indicate a highly significant effect (p-value$<$0.001) of water injection on the SFC of the engine. The results also confirm water injection's significant effect on power and NOx emissions (p-value$<$0.05). The statistical analysis indicates that varying biodiesel percentages significantly affect power output during water injection in the cylinder. Furthermore, the analysis of variance demonstrates a highly significant effect (p-value$<$0.001) of EGR on power output, SFC, and NOx emissions. Table 5 also shows that using biodiesel with EGR in the engine significantly affects power output, SFC, and NOx emissions. Overall, EGR exhibits a more significant effect on power than water injection. Both methods for SFC are equally effective; however, EGR has a higher impact on specific NOx emissions than water injection.

4. Conclusions

The findings of this study contributed directly to the advancement of green and sustainable transport by evaluating effective methods for reducing NOx emissions in diesel engines, a critical concern in minimizing environmental pollution. This study systematically compared two key NOx mitigation strategies -water injection and EGR -using numerical simulations on a Caterpillar 3406 diesel engine. The results highlight the potential of these techniques in significantly lowering NOx emissions, with EGR achieving a reduction of approximately 80 % and water injection reducing NOx emissions by around 60 %. Such decreases are vital for meeting stricter emissions standards and enhancing the sustainability of diesel-powered transport systems. The results of this investigation can be summarized as follows.

1. The size of the water droplets or the injector nozzle diameter significantly affects NOx production. This study specified the optimal droplet size as 0.18 mm, resulting in NOx production of 0.24 g/kW.hr.
2. Increasing the spray angle of water injection reduces NOx emissions due to the wider water jet despite the shorter penetration length. The lowest NOx production occurs at a spray angle of 16°.
3. Increasing the percentage of water injection and the EGR rate reduced the In-cylinder pressure and heat release rate across various fuel blends and CAs.
4. Due to the increased ignition delay caused by water injection and EGR, the peak heat release rate for higher water injection percentages and EGR rates occurred further from TDC.
5. As the percentage of water injection increased from 0 % to 45 %, the engine power decreased while SFC increased. However, at 60 % water injection, the indicated power slightly increased while the SFC decreased.
6. Increasing water injection up to 45 % reduces the maximum in-cylinder pressure by 4.4 % and engine power by 3.2 %–4.4 % for different fuel mixtures. However, a slight increase in power is observed when the water injection percentage reaches 60 %.
7. The SFC rises by 6.4 % during increasing water injection. Similarly, as the EGR rate increases, power declines by 3.5 %–4.3 %,

Table 4
Results of ANOVA-water injection.

	Power				SFC				Specific NOx			
Source	Adj SS	Adj MS	F-Value	P-Value	Adj SS	Adj MS	F-Value	P-Value	Adj SS	Adj MS	F-Value	P-Value
Water Injection (%)	4.939	1.235	13.44	0.0013	30033	7508.4	1094.4	<0.001	0.255	0.0638	234.7	0.0086
Biodiesel (%)	2.286	1.143	12.44	0.0035	114.6	57.29	8.35	0.011	0.0399	0.012	73.6	0.0012
Error	0.735	0.092	–	–	54.9	6.86	–	–	0.0022	0.0003	–	–
Total	7.96	–	–	–	30203	–	–	–	0.2971	–	–	–

Table 5
Results of ANOVA-EGR

	Power				SFC				Specific NOx			
Source	Adj SS	Adj MS	F-Value	P-Value	Adj SS	Adj MS	F-Value	P-Value	Adj SS	Adj MS	F-Value	P-Value
EGR (%)	3.133	0.783	33.17	<0.001	83.389	20.844	23.35	<0.001	0.606	0.152	126.1	<0.001
Biodiesel (%)	1.146	0.573	24.25	<0.001	52.204	26.1	29.24	<0.001	0.0515	0.026	21.4	<0.001
Residual	0.189	0.024	–	–	7.143	0.893	–	–	0.001	0.001	–	–
Total	4.468	–	–	–	142.7	–	–	–	0.667	–	–	–

comparable to the water injection scenario. Moreover, the SFC increases by 4.6 % across different fuel blends for the EGR case, although this increase is less than that observed with water injection.

8. Water injection of up to 60 % significantly reduced specific NOx emissions, with a decrease of approximately 57 %. In contrast, using EGR at 0–25 % reduced specific NOx emissions by approximately 78 %.
9. Increasing the biodiesel percentage in the fuel mixture has led to a 19 % and 17 % increase in specific NOx emissions for the EGR and water injection cases, respectively.
10. Overall, EGR significantly affects power more than water injection. Both methods for SFC are equally effective; however, EGR has a higher impact on specific NOx emissions than water injection.
11. Based on the results and considering engine performance and the reduction of nitrogen oxides with the two methods examined in this study, the EGR method is recommended over the water injection method.
12. Future research could investigate and compare the effects of different biofuels, including alcohols and water injection timing strategies, on combustion, performance characteristics, and NOx emissions in diesel engines. This approach could provide greater insight into the impact of water injection and alternative fuels.

CRediT authorship contribution statement

Maziyar Moeini Manesh: Writing – original draft, Software. **Alireza Shirneshan:** Writing – review & editing, Project administration, Methodology, Investigation. **Sobhan Emami:** Writing – review & editing, Software, Methodology.

Declaration of competing interest

The authors declare that they have no known competing financial interests or personal relationships that could have appeared to influence the work reported in this paper.

Data availability

No data was used for the research described in the article.

References

Alahmer, A., et al., 2010. Engine performance using emulsified diesel fuel. Energy Convers. Manag. 51 (8), 1708–1713.

Ayhan, V., 2020. Investigation of electronic controlled direct water injection for performance and emissions of a diesel engine running on sunflower oil methyl ester. Fuel 275, 117992.

Ayhan, V., Ece, Y.M., 2020. New application to reduce NOx emissions of diesel engines: electronically controlled direct water injection at compression stroke. Appl. Energy 260, 114328.

Chen, Z., et al., 2022. Exploring the potential of water injection (WI) in a high-load diesel engine under different fuel injection strategies. Energy 243, 123074.

Chintala, V., Subramanian, K.A., 2016. Experimental investigation of hydrogen energy share improvement in a compression ignition engine using water injection and compression ratio reduction. Energy Convers. Manag. 108, 106–119.

Co, A., 2014. Theory Guide, AVL FIRE, Version 2014.

De Poures, M.V., et al., 2017. 1-Hexanol as a sustainable biofuel in DI diesel engines and its effect on combustion and emissions under the influence of injection timing and exhaust gas recirculation (EGR). Appl. Therm. Eng. 113, 1505–1513.

Dodge, L.G., et al., 1996. A PC-based Model for predicting NOx Reductions in diesel engines. SAE International.

Duan, X., et al., 2021. Effects of injection timing and EGR on combustion and emissions characteristics of the diesel engine fuelled with acetone–butanol–ethanol/diesel blend fuels. Energy 231, 121069.

Dubey, A., et al., 2022. Combined effects of biodiesel − ULSD blends and EGR on performance and emissions of diesel engine using Response surface methodology (RSM). Energy Nexus 7, 100136.

Ergen, G., 2024. Comprehensive analysis of the effects of alternative fuels on diesel engine performance combustion and exhaust emissions: role of biodiesel, diethyl ether, and EGR. Therm. Sci. Eng. Prog. 47, 102307.

Farnham, C., N, M., Nabeshima, M., Mizuno, T., 2015. Effect of water temperature on evaporation of mist sprayed from a nozzle. J. Heat. Isl. Inst. Int 10.

Fayad, M.A., et al., 2022. Investigation the effect of fuel injection strategies on combustion and morphology characteristics of PM in modern diesel engine operated with oxygenate fuel blending. Therm. Sci. Eng. Prog. 35, 101476.

Fayad, M.A., et al., 2023. Reducing soot nanoparticles and NOX emissions in CRDI diesel engine by incorporating TiO2 nano-additives into biodiesel blends and using high rate of EGR. Energies 16. https://doi.org/10.3390/en16093921.

Gao, H., et al., 2016. A modification to the WAVE breakup model for evaporating diesel spray. Appl. Therm. Eng. 108, 555–566.

Ghaffarpour, M., Baranescu, R., 1996. NOx reduction using injection rate shaping and intercooling in diesel engines. SAE International.

Giakoumis, E.G., et al., 2012. Exhaust emissions of diesel engines operating under transient conditions with biodiesel fuel blends. Prog. Energy Combust. Sci. 38 (5), 691–715.

Hanjalić, K., Popovac, M., Hadžiabdić, M., 2004. A robust near-wall elliptic-relaxation eddy-viscosity turbulence model for CFD. Int. J. Heat Fluid Flow 25 (6), 1047–1051.

Hoekman, S.K., Robbins, C., 2012. Review of the effects of biodiesel on NOx emissions. Fuel Process. Technol. 96, 237–249.

Hojati, A., Shirneshan, A., 2019. Effect of compression ratio variation and waste cooking oil methyl ester on the combustion and emission characteristics of an engine. Energy Environ. 31 (7), 1257–1280.

Kumar, J.T.S., et al., 2018. Effect of reformed EGR on the performance and emissions of a diesel engine: a numerical study. Alex. Eng. J. 57 (2), 517–525.

Kumar Patidar, S., Raheman, H., 2020. Performance and durability analysis of a single-cylinder direct injection diesel engine operated with water emulsified biodiesel-diesel fuel blend. Fuel 273, 117779.

Mobasheri, R., Peng, Z., Mirsalim, S.M., 2012. Analysis the effect of advanced injection strategies on engine performance and pollutant emissions in a heavy duty DI-diesel engine by CFD modeling. Int. J. Heat Fluid Flow 33 (1), 59–69.

Moon, S., et al., 2010. Improving diesel mixture preparation by optimization of orifice arrangements in a group-hole nozzle. Int. J. Engine Res. 11, 109–126.

Nehmer, D.A., Reitz, R.D., 1994. Measurement of the effect of injection rate and split injections on diesel engine soot and NOx emissions. SAE International.

Park, S.H., Youn, I.M., Lee, C.S., 2011. Influence of ethanol blends on the combustion performance and exhaust emission characteristics of a four-cylinder diesel engine at various engine loads and injection timings. Fuel 90 (2), 748–755.
Plee, S.L., Ahmad, T., Myers, J.P., 1981. Flame temperature Correlation for the Effects of exhaust gas Recirculation on diesel Particulate and NO $_x$ emissions. SAE International.
Popovac, M., Hanjalic, K., 2007. Compound wall treatment for RANS computation of complex turbulent flows and heat transfer. Flow Turbul. Combust. 78 (2), 177–202.
Qi, D., et al., 2021. Effects of EGR rate on the combustion and emission characteristics of diesel-palm oil-ethanol ternary blends used in a CRDI diesel engine with double injection strategy. Appl. Therm. Eng. 199, 117530.
Radheshyam, K. Santhosh, Kumar, G.N., 2020. Effect of 1-pentanol addition and EGR on the combustion, performance and emission characteristic of a CRDI diesel engine. Renew. Energy 145, 925–936.
Rajesh Kumar, B., et al., 2016. Combined effect of injection timing and exhaust gas recirculation (EGR) on performance and emissions of a DI diesel engine fuelled with next-generation advanced biofuel – diesel blends using response surface methodology. Energy Convers. Manag. 123, 470–486.
Ramesh, N., Mallikarjuna, J.M., 2017. Low temperature combustion strategy in an off-highway diesel engine – experimental and CFD study. Appl. Therm. Eng. 124, 844–854.
Raut, A.A., Mallikarjuna, J.M., 2019. Effects of direct water injection and injector configurations on performance and emission characteristics of a gasoline direct injection engine: a computational fluid dynamics analysis. Int. J. Engine Res. 21 (8), 1520–1540.
Şahin, Z., Tuti, M., Durgun, O., 2014. Experimental investigation of the effects of water adding to the intake air on the engine performance and exhaust emissions in a DI automotive diesel engine. Fuel 115, 884–895.
Sandeep, S., et al., 2019. Assessment of water Injection in a heavy duty diesel Engine for NO $_x$ reduction potential. SAE International.
Shirneshan, A.R., et al., 2014. Investigating the effects of biodiesel from waste cooking oil and engine operating conditions on the diesel engine performance by response surface methodology. Iran. J. Sci. Technol. - Trans. Mech. Eng. 38 (M2), 289–301.
Soni, D.K., Gupta, R., 2016. Numerical investigation of emission reduction techniques applied on methanol blended diesel engine. Alex. Eng. J. 55 (2), 1867–1879.
Sun, X., et al., 2022. Effect of direct water injection on combustion and emissions characteristics of marine diesel engines. Fuel 309, 122213.
Taghavifar, H., Anvari, S., Parvishi, A., 2017. Benchmarking of water injection in a hydrogen-fueled diesel engine to reduce emissions. Int. J. Hydrogen Energy 42 (16), 11962–11975.
Taghavifar, H., Anvari, S., 2019. The effect of temperature and amount of water in co-injection of diesel-water on exergy and irreversibility rate of VGT diesel engine. Appl. Therm. Eng. 162, 114314.
Tesfa, B., et al., 2012. Water injection effects on the performance and emission characteristics of a CI engine operating with biodiesel. Renew. Energy 37 (1), 333–344.
Wei, J., et al., 2022. Physicochemical properties and oxidation reactivity of exhaust soot from a modern diesel engine: effect of oxyfuel type. Combust. Flame 238, 111940.
Yasin, M.H.M., et al., 2015. Effects of exhaust gas recirculation (EGR) on a diesel engine fuelled with palm-biodiesel. Energy Proc. 75, 30–36.
Zeldovich, Y.A., Frank-Kamenetskii, D., Sadovnikov, P., 1947. Oxidation of Nitrogen in Combustion. Publishing House of the Acad of Sciences of USSR.
Zhang, Z., et al., 2019. Effects of low-level water addition on spray, combustion and emission characteristics of a medium speed diesel engine fueled with biodiesel fuel. Fuel 239, 245–262.
Zhang, Z., et al., 2021. The effects of Fe2O3 based DOC and SCR catalyst on the combustion and emission characteristics of a diesel engine fueled with biodiesel. Fuel 290, 120039.
Zhou, D.Z., et al., 2015. Application of CFD-chemical kinetics approach in detecting RCCI engine knocking fuelled with biodiesel/methanol. Appl. Energy 145, 255–264.